

New Physics Searches

Gustaaf Brooijmans

Columbia University, New York, USA

1 Introduction

At the time of this writing, all experimental results are consistent with a model of particle physics which contains six quarks (up, down, charm, strange, top and bottom) and six leptons (electron neutrino, electron, muon neutrino, muon, tau neutrino and tau). The properties of these particle, with the exception of the neutrino masses, have been measured accurately, and the standard model describes their weak, electromagnetic and strong interactions as mediated by the W and Z bosons, photons and gluons respectively with remarkable accuracy (The LEP and SLD Collaborations, 2006). Lacking in this description are a consistent quantum theory of the gravitational interaction, and any understanding of the pattern suggested by the properties of the fermions.

Many questions thus remain to be answered, e.g. what is spin or color or electric charge? Are these static “properties” of particles, or do they result from a hidden dynamic? Are there only three generations? Why are there for example no neutral, colored fermions? What is the link between particle and nucleon masses?

There is also one known problem in the standard model: at a center-of-mass energy of 1.7 TeV, the longitudinal W boson scattering cross-section violates the unitarity bound (Lee et al., 1977)¹. One solution to this problem is the introduction of the so-called Higgs boson (Higgs, 1964a; Higgs, 1964b; Higgs, 1966; Englert and Brout, 1964; Guralnik et al., 1964), which in the standard model can also generate the fermion masses. The latter allows the decoupling of the mechanism responsible for fermion masses from the standard model interactions. However, quadratically divergent radiative corrections suggest the standard model Higgs boson mass is close to the limit of validity of the theory, and experimental constraints (Alcaraz et al., 2007) imply its

¹A second problem is with the $f\bar{f} \rightarrow W^+W^-$ cross-section, but this is less severe and is also addressed by the standard model Higgs boson.

mass is less than approximately 200 GeV. This suggests the scale of new physics is at or below 1 TeV, although in principle, if one accepts a high level of fine-tuning, with the addition of a $m_H \approx 150$ GeV Higgs boson the list of existing particles could be “complete”, in analogy with Mendeleev’s table in chemistry. No new physics would then appear below the Planck scale of 10^{19} GeV. This would of course be a very unsatisfactory outcome, as it would not help us answer any questions as to the nature of the fermions. The high degree of fine-tuning needed in this scenario is a strong motivation for the presence of new particles and/or interactions at or just above the electroweak scale.

2 Unravelling the Mystery: the Tools

Assuming that there is indeed new physics to help us understand the observed patterns, then the path to its discovery goes through both the collection of additional information (experiments), and searching for the underlying pattern (theory). Experimental searches for new physics can broadly be categorized into a) precision measurements of particle properties and interactions in searches for deviations from standard model predictions, and b) searches for new particles or interactions in new areas in “phase space,” typically energy domains that have not yet been probed. On the theoretical front, hypotheses lead to models whose internal consistency as well as compatibility with existing data needs to be verified, and if confirmed leads to new suggestions on where to look. Given the time available, these lectures will focus on the experimental search for new physics at the energy frontier.

The new physics must couple to the standard model in some way, but the lack of any deviations so far implies that that coupling must be either weak or hidden through some mechanism, for example near-cancellation of competing amplitudes. It could be “standard model-like” in the sense that it consists of new short-lived, massive particles decaying to known fermions or bosons, or there might be some new longer-lived particles with unusual properties, or no new particles may be in reach, but new interactions might manifest themselves. The situation may even be more extreme and the concept of “particles” or “interactions” may need to be replaced by a fundamentally different paradigm. In any case, the number of possibilities is certainly too vast to explore here, and in the following it is the search for anomalous production of standard model particles, in either resonant or non-resonant mode by short-lived new particles that will be discussed. While in many cases this can be done in a model-independent way, it is important to keep the implications of known constraints in mind, and to understand that some scenarios require the development of new experimental techniques.

The tools used in the searches that will be described are the Fermilab Tevatron and CERN LHC, proton-(anti)proton colliders at 1.96 and 7–14

TeV respectively. Since these are hadron colliders, the incoming longitudinal² momentum of the quarks and/or gluons engaged in the “hard” (large $\sqrt{\hat{s}}$) scatter is not known, and the large momentum of these particles leads to a Lorentz contraction in the lab frame of all distances in the longitudinal direction. For these two reasons, most selections are based on quantities measured in the transverse direction, and the larger the $\sqrt{\hat{s}}$, the more “central” the events will be in the detector. The detectors are designed to make the best possible measurements of all particles produced in the collisions. A detailed description of the detectors installed at the LHC is given elsewhere in this volume. The Tevatron detectors, CDF and DØ, are very similar.

3 The Higgs Hunt

The search for the Higgs boson at the Tevatron will be used to give a detailed description of the experimental techniques used in the search for new physics. This is an interesting example since it is a search for a small signal in a large background dominated by vector boson plus jets events, and thus requires the use of the most advanced tools on both the experimental and theoretical fronts.

The Higgs boson production cross-section at the Tevatron ranges from approx. 1 ($m_H = 120$ GeV) to 0.3 pb ($m_H = 180$ GeV) in the gluon fusion channel, and 0.2 ($m_H = 120$ GeV) to 0.03 pb ($m_H = 180$ GeV) for production in association with a vector boson. At the lower end of this mass region the Higgs boson dominantly decays to a $b\bar{b}$ pair, so that in the face of the overwhelming QCD production of $b\bar{b}$ events, only Higgs bosons produced in association with vector bosons (which themselves decay leptonically) are detectable. At higher mass, where decays to a W^+W^- pair become sizable, the higher rate gluon fusion process becomes viable provided at least one of the W bosons decays leptonically. Since each experiment has collected about 7 fb^{-1} of data, the total number of detectable Higgs bosons that have been produced is at best a few thousand. Decays with small branching ratios are thus not accessible at the Tevatron.

3.1 Dilepton Plus Missing Transverse Energy Channel

$H \rightarrow W^+W^- \rightarrow \ell^+\nu\ell^-\nu$ decays, where ℓ represents an electron or a muon, form the “golden channel” at the Tevatron: the main background, $Z \rightarrow \ell^+\ell^-$ is also a great reference signal to determine efficiencies and the sample composition, and the missing transverse energy (\cancel{E}_T) present in the signal provides an excellent means to suppress the Z boson contribution. Both the dilepton invariant mass and \cancel{E}_T are shown at preselection level in Fig.1 for the most recent DØ search (The DØ Collaboration, 2009a). After the preselection, which

²Longitudinal and transverse denote directions w.r.t. the direction of the incoming colliding beams.

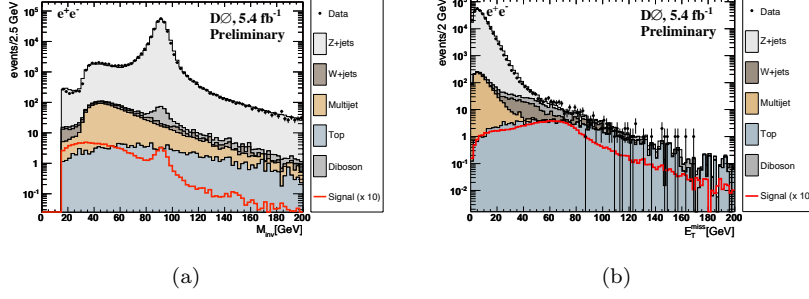


Figure 1. (a) Dielectron invariant mass and (b) missing transverse energy at the preselection level in the $D\bar{O}$ search for the Higgs boson in the dilepton plus missing transverse energy channel.

mainly consists of requiring the presence of two good quality charged leptons (electrons or muons) with transverse momentum (p_T) greater than 10 (15) GeV for muons (electrons) and invariant mass larger than 15 GeV, cuts are applied to enhance the signal/background ratio. These selection cuts are applied on the following variables: \cancel{E}_T , scaled \cancel{E}_T (which is a measure of the probability that the \cancel{E}_T originates from poor measurement of other objects in the event), $M_T^{\text{min}}(\ell, \cancel{E}_T)$, the minimum of the transverse masses calculated from each of the charged leptons and the \cancel{E}_T , and $\Delta\phi(\ell, \ell)$, the azimuthal angle between the charged leptons. Two of these variables, $M_T^{\text{min}}(\ell, \cancel{E}_T)$ and $\Delta\phi(\ell, \ell)$ are illustrated at preselection level in Fig.2.

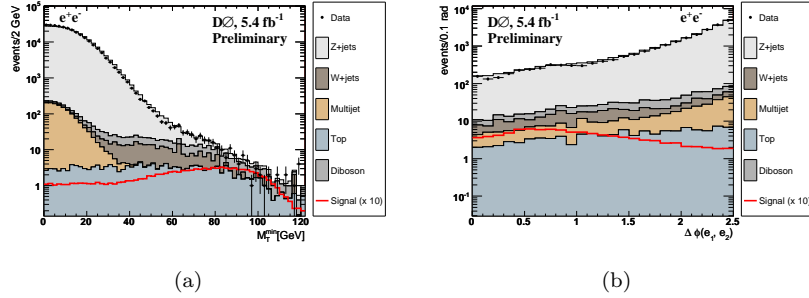


Figure 2. (a) Minimum transverse mass and (b) azimuthal angle between the leptons at preselection level in the $D\bar{O}$ search for the Higgs boson in the dilepton plus missing transverse energy channel.

After the enhancement cuts, the signal/background ratio is still relatively small (1/30, 1/50 and 1/1000 in the $e\mu$, ee and $\mu\mu$ channels respectively.) While this could be improved further, cuts are left loose since optimization is done in a next step: multivariate tools are used to exploit the different correlations between variables for signal and background. In this particular

analysis, 14 variables with good agreement between data and expectation, based on lepton transverse momenta, \cancel{E}_T and the angles between these, are injected into a neural network for each of the three channels. The neural network output distributions are then combined into one (Fig.3), and in the absence of signal that distribution will be used to set a limit on the Higgs boson production cross-section.

The systematic uncertainties are propagated through the full analysis chain to the neural network output distribution: the analysis is repeated with, for example, the jet energy scale shifted up, then down by one standard deviation. Some of these uncertainties, like the jet reconstruction efficiency, affect the shape of the distribution, while others such as the uncertainty on the integrated luminosity, affects the normalization only. The uncertainties are treated as nuisance parameters which are generally correlated, but not at the 100% level, between different background contributions. These uncertainties are often only known with moderate accuracy, and the data can be used to further constrain them. To do this, pseudo-experiments are produced by generating events for each of the neural network output distribution's bins according to a Poisson distribution, with mean equal to the number of expected events. For each pseudo-experiment, the nuisance parameters are then varied within the expected range, leading to variations in both the signal and signal+background distributions. The results can then be compared to the data using a log-likelihood ratio, which can be maximized as a function of the nuisance parameters, effectively constraining their values. Basically, the full shape of the neural network output distribution is used to “profile” the systematics, in other words determine which background uncertainties are over- or underestimated. Bins with large signal/background ratio can be removed to avoid any signal-induced bias.

Finally, the full shape of the neural network output distribution is compared to both background and signal+background templates, including all uncertainties, to determine the limit on the Higgs boson production cross-section. This is usually shown as a ratio to the standard model prediction, so that the region where the observed limit curve is below one is excluded at 95% C.L. Both the neural network output distribution and limit are shown in Fig.3.

3.2 Lepton Plus Jets Channel

The final state consisting of a W boson (decaying to $\ell\nu$) plus two jets is critical at both low ($WH \rightarrow \ell\nu b\bar{b}$) and high mass ($H \rightarrow WW \rightarrow \ell\nu jj$.) In the former case we have $m_{b\bar{b}} = m_H$, and in the latter $m_{jj} = m_W$ and $m_{WW} = m_H$. However, the dijet mass resolution is intrinsically much worse than the dilepton mass resolution, and the backgrounds are substantially larger than in the dilepton channel.

In this case, the sample composition after preselection (typically one good lepton with $p_T > 20$ GeV, $\cancel{E}_T > 20$ GeV and two jets with $p_T > 20$ GeV) is

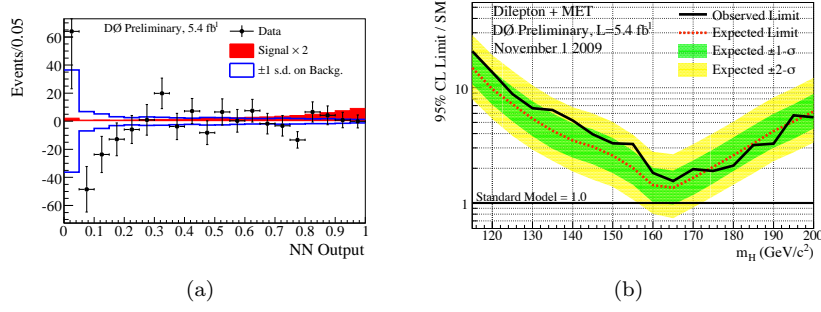


Figure 3. (a) Neural network output distribution, and (b) limit on the Higgs boson production cross-section in units of the standard model prediction (b) for the DØ search for the Higgs boson in the dilepton plus missing transverse energy channel.

more difficult to determine.

- The contributions from diboson and top quark production are taken from Monte-Carlo (MC) simulation since they are both relatively small, and 10%-level uncertainties on these backgrounds have a small impact.
- The contamination from the instrumental QCD multijet background in which one jet is misidentified as a lepton is evaluated directly from the data.
- The Z boson plus jets component is taken from a simulated sample which is corrected based on direct measurements: indeed, as we will see, the difference between the simulation and observation is significant.
- For the major background, W boson plus jets production, simulation is also used, but here the correction to be applied is much harder to determine, in part due to the potential signal contamination. In principle, corrections determined from the Z boson plus jets sample can be mapped to W boson plus jets after correcting for vector boson mass effects, but in practice the correlation between variables makes this highly non-trivial.

Four types of MC generators are used:

- “Calculators” implement (up to next-to-next-to-leading-order) calculations of specific quantities, for example boson p_T distributions. Two commonly used generators of this type are RESBOS (Balazs and Yuan, 1997) and MCFM (Campbell and Ellis, 2002). These calculators do not generate complete events.
- Traditional $2 \rightarrow 2$ generators like PYTHIA (Sjostrand et al., 2006) or HERWIG (Corcella et al., 2001) implement leading order calculations

of many $2 \rightarrow 2$ processes (e.g. $q\bar{q} \rightarrow e\nu$, and include a parton shower (PS) model and hadronization, thus allowing the generation of complete events that can be fed into a detector simulation. Any jets beyond those from the $2 \rightarrow 2$ matrix element are produced at the parton shower stage.

- “Matrix Element” generators allow the generation of $2 \rightarrow n$ ($n < 9$) events (e.g. $q\bar{q} \rightarrow e\nu jjjj$). The calculations are also done at leading order, but these generators are necessary to simulate events with multiple hard jets. Care needs to be taken not to “double count” events in which additional jets are produced during the parton shower stage. Two approaches exist to handle this: the CKKW method implemented in SHERPA (Gleisberg et al., 2009) and the MLM method used in ALPGEN (Mangano et al., 2003).
- “NLOwPS” $2 \rightarrow 2$ generators include next-to-leading order corrections, so in a sense are $2 \rightarrow 3$ generators with virtual corrections. The two generators of this type that are in use are MC@NLO (Frixione and Webber, 2002) and POWHEG (Frixione et al., 2007).

In the case of the Higgs boson search in the W boson plus jets channel, the matrix element generators are used to simulate the dominant background, but this simulation needs to be “corrected” to address modeling deficiencies arising from non-perturbative effects, their leading order nature, and other aspects for which our understanding is limited, for example the underlying event contribution. The magnitude of these necessary corrections can be estimated from a comparison of Z boson plus jets data to simulated samples. Two example distributions from a $D\bar{O}$ analysis (Abazov et al., 2008a) are given in Fig. 4.

After the W boson plus jets events produced with ALPGEN have been reweighted using distributions obtained from RESBOS (for the boson p_T) and SHERPA (for the jet angular distributions), good agreement between data and simulation is obtained. The search is then optimized using multivariate tools, and the so-called matrix element technique. This approach, which was successfully used in measuring the top quark mass and observation of single top quark production, is basically an unbinned maximum likelihood fit that gives extra weight to more signal-like events: for each event, signal and background probabilities are calculated based on the compatibility of the physics object (leptons and jets) four-vectors with the process under study. The output of the matrix element calculation is used as an additional input to a neural network, and boosts the sensitivity by 5%, equivalent to an increase in the data set size by 10%.

3.3 Current Result

In the end, 90 mutually exclusive final states are analyzed by CDF and $D\bar{O}$ and combined to produce a Tevatron limit on standard model Higgs boson

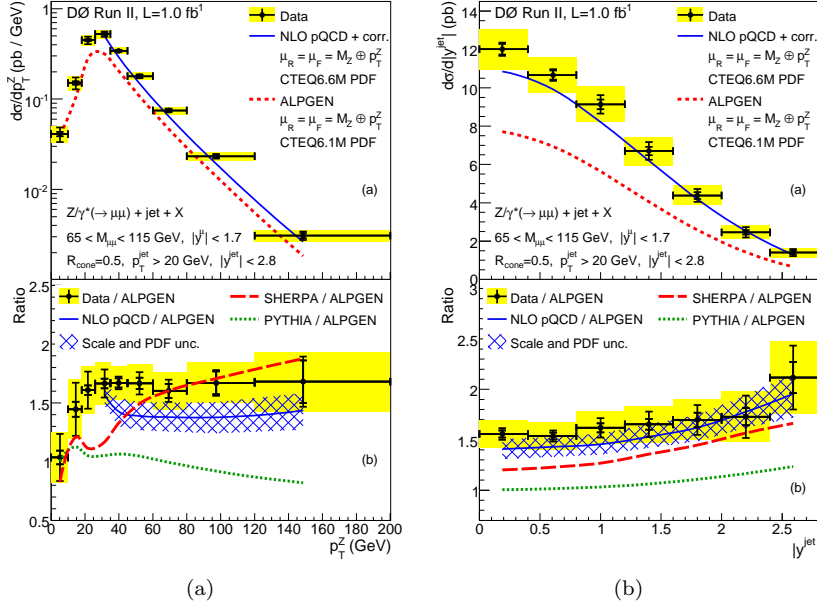


Figure 4. Comparison of Z boson plus jets data with the prediction from various generators after unfolding of detector effects, i.e. at particle level: (a) Z boson p_T and (b) leading jet rapidity distributions. The curve denoted “NLO pQCD” was produced using MCFM.

production (The CDF and DØ Collaborations, 2009). The result at the time of this writing is shown in Fig. 5, and excludes the existence of a standard model Higgs boson with mass $163 < m_H < 166$ GeV.

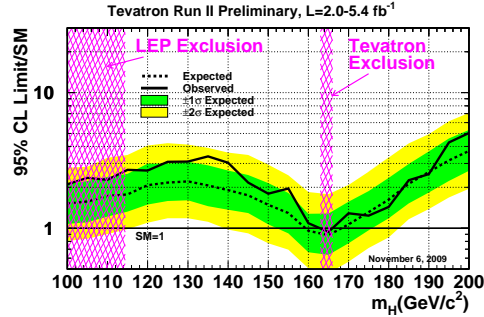


Figure 5. Combination of the CDF and DØ results in the search for a standard model Higgs boson.

4 Searches for Supersymmetry

The existence of new particles with masses close to the Higgs boson mass could be an effective way to cancel out the quadratically divergent loop corrections to the latter. In supersymmetry, for every standard model fermion (boson) there is a partner boson (fermion), so that the quadratically divergent diagrams are naturally canceled by their supersymmetric counterparts. “Little Higgs” models take a similar approach, except that partners only exist for the worst offenders – the top quark, W , Z and Higgs bosons – and other new physics is expected to exist at the 10 TeV scale.

Even in the minimal supersymmetric standard model (MSSM), which has the minimal set of supersymmetric particles, there are 105 new free parameters, and the simplest searches performed in this context make a number of basic assumptions: R -parity is conserved so that superpartners are pair-produced (or in some cases explicitly violated and single particle production is considered;) the pair-produced superpartners typically each decay to their standard model partner and the lightest supersymmetric particle (LSP), leading to signatures with a pair of jets or leptons and missing (transverse) energy. Results are then presented as limits in the superpartner-LSP mass plane. In this scenario, searches by the LEP II experiments set limits on superpartner masses that are in the range from 90 to 100 GeV, very close to the kinematic limit, and cover just about all of the allowed $(m_{\text{superpartner}}, m_{\text{LSP}})$ plane below that. Tevatron experiments have a larger kinematic reach (typically ~ 200 GeV in superpartner mass), but are typically not sensitive in the band $m_{\text{superpartner}} - m_{\text{LSP}} \leq 15$ GeV.

An exception to the two-body decay case is the pair production of top squarks at the Tevatron. If the top squark is lighter than the top quark then the three-body decay to a bottom quark, a lepton and an LSP sneutrino becomes dominant. The final state differs from the dilepton signature of $t\bar{t}$ decays only in the kinematics, with potentially very small lepton p_T values if the mass difference between the top squark and the sneutrino is small. This can be seen in the left panel of Fig. 6 which shows the electron p_T spectrum in the $D\bar{O}$ search for the top squark in the $e\mu\cancel{E}_T$ channel (The D0 Collaboration, 2009b). The cut-based analysis has low background so that no explicit cut on the number of jets is required, leading to the excluded region given in the right panel of Fig 6, which also illustrates the contrast between LEP and Tevatron searches in probing the small $m_{\text{superpartner}} - m_{\text{LSP}}$ region.

Supersymmetry is manifestly broken, since the superpartner masses differ from the standard model particle masses, and various breaking models have been developed. These lead to predictions for superpartner mass hierarchies and the nature of the LSP, thus predicting specific experimental signatures. An added bonus is that in most of these breaking models, the μ^2 term in the Higgs potential is driven negative for a large fraction of parameter space when run down from the GUT to the electroweak scale, thus explaining electroweak symmetry breaking. This is however driven by the large value of the (in

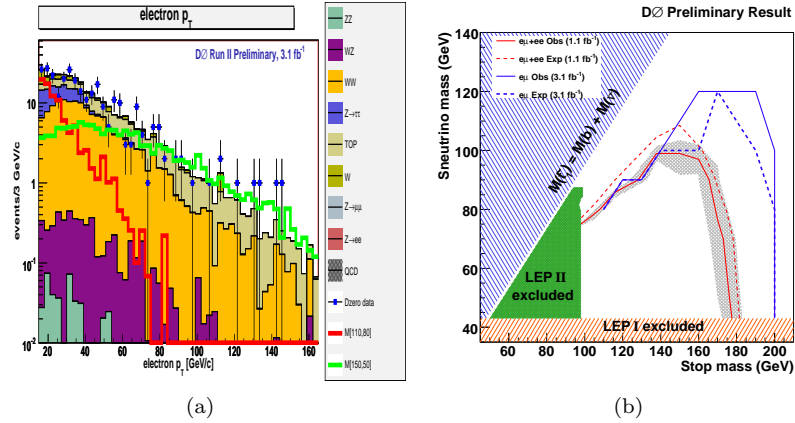


Figure 6. Search for top squarks in $e\mu\cancel{E}_T$ events by DØ: (a) electron p_T distribution and (b) excluded region in the sneutrino-stop mass plane.

principle arbitrary) top quark mass.

In the vast majority of these models, strongly interacting superpartners (squarks and gluinos) are substantially heavier than the sleptons and electroweak gauginos, but at hadron colliders this is usually more than compensated for by the larger interaction strength. If they are within the kinematical reach, the produced squarks and gluinos will decay to quarks, gluons and LSPs, leading to a final state consisting of jets and \cancel{E}_T . This is a difficult experimental signature, since most collisions lead to jets, most detector malfunctions will lead to \cancel{E}_T , and the jet energy resolution is intrinsically limited given the large fraction of invisible energy jets deposit. Searches in this final state therefore require close attention to data quality, both on- and offline, but since some noise sources will manifest themselves very infrequently, continuous feedback from the analysis to online operations is a necessity. From past experience, some effects only lead to a few anomalous events per year.

The search sensitivity is as always maximized by treating different final states separately, with specific optimizations of the background suppression cuts. Whereas squarks typically decay to a quark and an LSP, gluinos decay to a squark and a quark yielding a $q\bar{q}$ LSP final state. Pair production of squarks then leads to a dijet plus \cancel{E}_T signature, and pair production of gluinos to four jets plus \cancel{E}_T . Associated production of a squark with a gluino is also possible giving the three jets plus \cancel{E}_T final state. The recent DØ search (Abazov et al., 2008d) treats each channel separately starting at the trigger level. The instrumental QCD multijet background is suppressed requiring that the \cancel{E}_T not be aligned with any of the jets in the azimuthal plane, and the dominant physics backgrounds are $Z(\rightarrow \nu\nu) + jets$, $W(\rightarrow \ell\nu) + jets$ and $t\bar{t}$ production. Figure 7 shows the \cancel{E}_T distribution in the two jet channel, and the obtained result interpreted in the minimal supergravity (mSUGRA) model. Note that

the exclusion reaches further in m_0 than $m_{1/2}$, showing the better sensitivity to squarks than gluinos.

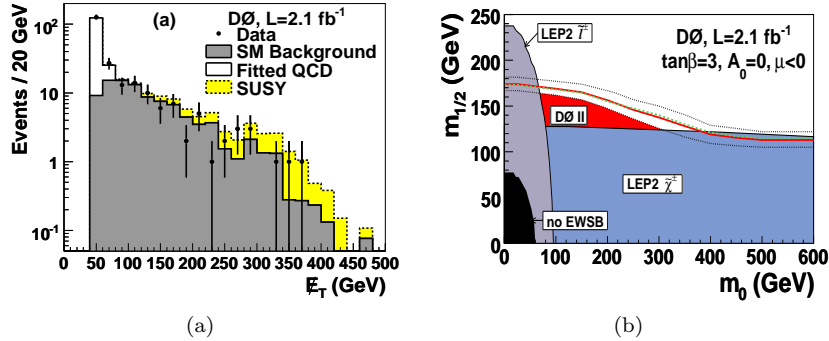


Figure 7. Search for squarks and gluinos in the jets plus E_T channel by $DØ$: (a) E_T distribution in the two-jet channel and (b) excluded region in the $mSUGRA$ interpretation.

If the colored superpartners are out of kinematical reach, the search for electroweak gaugino pair production is the most promising avenue for discovery at hadron colliders. This can lead to a spectacular trilepton signature, which has an enhanced rate if the sleptons are light enough to mediate the chargino or neutralino decays: charginos (neutralinos) then decay to a slepton and neutrino (charged lepton), with the slepton subsequently decaying to a charged lepton and LSP. The cross-section is of course small, but so are the backgrounds from pair production of weak vector bosons. In fact, the backgrounds are so small that only two well-identified charged leptons are required, and an isolated track is taken as a candidate for the third. The main difficulty comes from the fact that the mass splittings between the involved supersymmetric particles are presumably small, so that the charged leptons produced in the decays are relatively soft. Figure 8 shows the track transverse momentum distribution in the $e\mu l$ channel (where l can be any charged lepton, identified as an isolated track) and the excluded $mSUGRA$ region in a recent $DØ$ analysis (Abazov et al., 2009a) combining multiple final states. Note that in contrast to the squark and gluino search, this analysis is more sensitive in $m_{1/2}$ than m_0 , since it searches for SUSY fermions.

The LHC reach for supersymmetric particles will go up to about 4 TeV in m_0 and 1400 GeV in $m_{1/2}$. If supersymmetry is to provide us with an efficient cancellation of the Higgs mass corrections' quadratic divergences and a good dark matter candidate, it will therefore need to be particularly finetuned to escape detection for another decade. If SUSY is found however, the prospects for measuring its mass spectrum and learning about the way supersymmetry is broken are good, even with LSPs escaping undetected in every event. Kinematic endpoints and new variables like m_{T2} (Lester and Summers, 1999) or

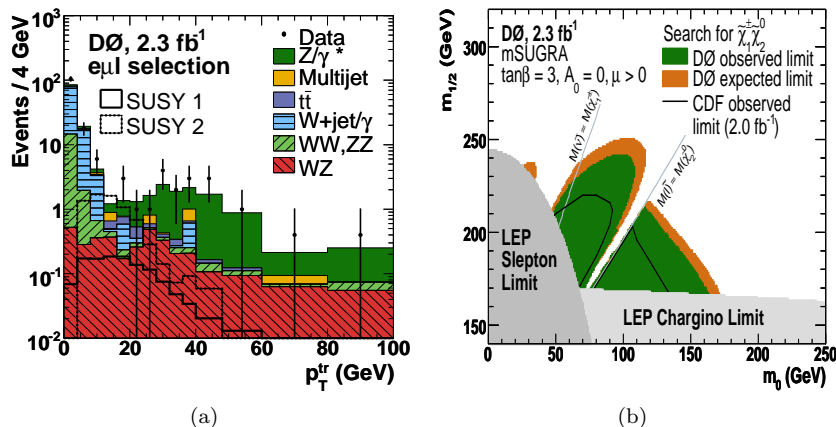


Figure 8. Search for associated production of charginos and neutralinos in trilepton events by $D\bar{O}$: (a) track p_T distribution in the $e\mu l$ channel and (b) excluded region in the $mSUGRA$ interpretation.

the contranverse mass (Polesello and Tovey, 2009) have been shown to be very powerful for such measurements.

Supersymmetric theories have a number of very attractive features: they explain the low Higgs boson mass (and sometimes electroweak symmetry breaking), lead to gauge coupling unification at a high scale, feature a candidate dark matter particle, and all of this without the need to introduce new interactions. However, this also comes at a large cost: many new particles are needed with a correspondingly large number of new free parameters, and no answers are given for any questions regarding the nature of particles. Parallels can certainly be drawn between expecting the presence of low scale supersymmetry and dinosaurs on Venus (Sagan, 1980).

5 New Gauge Bosons and Parity Restoration

Our assignments of fermions to generations are based on the subjective criteria of mass ordering and keeping the Cabibbo-Kobayashi-Maskawa matrix as diagonal as possible. If we accept this classification however, it becomes apparent that within a generation, the more a fermion interacts, the heavier it is (with the exception of the up and down quarks for which mass is an ill-defined concept.) This pattern suggests that fermion masses may have their origin in a more complex mechanism with an indirect relation to the standard model interactions, as for superpartner masses in gauge mediated supersymmetry breaking scenarios for example. The Higgs boson may then only be relevant to regulate the longitudinal vector boson cross-section, relaxing existing mass constraints and limits.

The difficulty with fermion masses in the standard model of course originates in the purely left-handed nature of the weak interaction, since massive fermions can change helicity. A deeper understanding of spin would be a major step forward, but there is as yet no indication as to the scale at which any hints in that direction might reveal themselves. A related phenomenon would be a step towards the restoration of parity symmetry.

The primary signals of parity restoration are of course the existence of a heavy right-handed W' boson and corresponding Z' boson, although the couplings need not be purely right-handed. Dilepton decays of these offer clean signals with well-understood backgrounds, and although there is some concern about determining the energy scale for very high p_T leptons at the LHC, the different dependence of electron and muon energy/momentum resolution as a function of p_T should offer a good handle. As opposed to the standard model W and Z bosons, $t\bar{t}$ decays should also be present and observable, and decays to a right-handed neutrino ν_R may be important if it is light enough. Beyond parity restoration, many models in fact predict the existence of Z' bosons (Langacker, 2008).

Z' boson production at the Tevatron and LHC mainly comes from up and down quarks, with model-dependent couplings determining the cross-section and width (Rizzo, 2006). The decays are somewhat similar to the standard model Z boson, but the branching fraction to light neutrinos is presumably suppressed while the $t\bar{t}$ channel opens up and $\nu_R\bar{\nu}_R$ may exist. The most promising channel for discovery is $Z' \rightarrow ee$ since the electron energy resolution at high p_T is dominated by the constant term, leading to a typical value of 10 GeV at 1.5 TeV. This is sufficiently good to be able to measure the Z' boson width in many models. The LHC will possibly extend the Tevatron reach (~ 1 TeV) in 2010 already, since the Z boson peak offers an excellent analysis calibration reference and the backgrounds are typically very low. A recent study of the ATLAS sensitivity (Aad et al., 2009) at $\sqrt{s} = 14$ TeV is shown in the left panel of Fig. 9. Note that at 10 TeV, the Z' boson production cross-section is typically about a factor of two smaller. Many searches for resonances are done by counting events in a shifting mass window, leading to the so-called “look elsewhere” effect: an excess will always be found if a sufficient number of distributions is studied. A better approach is to perform a global fit to the Drell-Yan spectrum, with an added gaussian of free amplitude and width, thus allowing the fit to find the mass. This type of “shape” analysis is naturally more sensitive, but not immune to the look elsewhere effect: in all cases, pseudo experiments should be run to determine the sensitivity of the experiment or quantify the magnitude of an excess. The current limits on Z' boson masses from CDF (Aaltonen et al., 2009a) are shown in the right panel of Fig. 9. If a new high mass dielectron resonance is found, the study of the angle between the lepton and the beam direction will be very valuable in determining its spin, since spin 1 particles tend to emit leptons closer to the beam. However, experimental acceptance effects largely negate this, because lepton identification in the forward region is significantly more difficult and

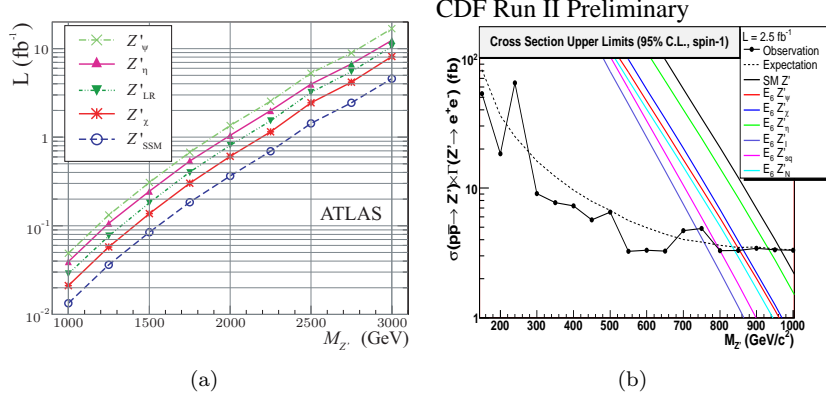


Figure 9. (a) Sensitivity of the ATLAS experiment to a new Z' boson as a function of luminosity for various models at $\sqrt{s} = 14$ TeV. (b) The current limits on Z' bosons from CDF.

suffers from larger backgrounds.

It is generally possible to look for a new resonance in the dijet channel as well: while the backgrounds are manifestly much larger, good sensitivity can be reached (Abazov et al., 2004; Aaltonen et al., 2009b). For Z' bosons, the sensitivity is generally inferior to the leptonic channels however (Henriques and Poggioli, 1992). If the ν_R is lighter than $m_{Z'}/2$ then the $\nu_R \bar{\nu}_R$ decay channel opens up. This is presumably followed by $\nu_R \rightarrow l W_R^*$ and $W_R^* \rightarrow q \bar{q}$ leading to a signature with two charged leptons and four jets, or more leptons if for example $m_{\nu_R'} < m_{\nu_R}$ and more complex cascades open up. The ultimate LHC sensitivity to such scenarios is $m_{Z'} \approx 4$ TeV and $m_{\nu_R} \approx 1$ TeV (Ferrari and Collot, 2000). Note that if $m_{\nu_R} \ll m_{Z'}$, the lepton and jets from the ν_R decay could be collimated. New approaches to such situations will be discussed later.

The W' boson production rate is not very sensitive to its couplings (Rizzo, 2007), but the interference with the standard model W boson, neglected in most experimental studies, is key in identifying the W' boson coupling helicity. Of course, the absence of $W' \rightarrow l \nu$ decays, as expected in the purely right-handed case, would also provide an important indication! The standard transverse mass distribution can be used to search for $\ell \nu$ decays, with a sensitivity reaching 5 TeV at the LHC (de Roeck et al., 2006). An interesting alternative is to search for the decay $W' \rightarrow W Z$: at low-to-moderate mass where there is some background, the trilepton channel is the most sensitive, whereas for higher masses the semileptonic channels, where one of the W or Z bosons is allowed to decay hadronically, dominate. The Tevatron reach is expected to be somewhat below $m_{W'} = 1$ TeV for $BR(W' \rightarrow W Z) = 1\%$, and the LHC should be able to probe masses close to 3 TeV. It should be noted that in the semileptonic channel, for $m_{W'} > \sim 600$ GeV, the quarks

from the hadronically decaying vector boson are sufficiently collimated to be reconstructed as a single jet. Techniques to handle this will be discussed below. Of course, the $W' \rightarrow tb$ channel is also possible, and would be very valuable in determining branching ratios. The current Tevatron limits impose $m_{W'} > \sim 800$ GeV (Aaltonen et al., 2009c; Abazov et al., 2008e).

In general, if extra gauge bosons exist new exotic fermions are needed to cancel anomalies (Langacker, 2008). Such quarks or leptons could be pair-produced, followed by decays to weak vector bosons and standard model quarks or leptons. The LHC mass reach for such quarks should be in excess of 1 TeV (Mehdiyev et al., 2008).

6 Gravity and Hierarchy

A promising approach to quantum gravity consists in adding space dimensions: this is string theory. The additional space dimensions are then hidden, presumably because they are “compactified” in some way. The radius of compactification was usually assumed to be at the scale of gravity, $\sim 10^{18}$ GeV, until it was realized it could be as low as 1 TeV (Antoniadis, 1990).

6.1 ADD

In the ADD large extra dimension scenario developed in 1998 (Arkani-Hamed et al., 1998), the standard model fields are confined to a 3+1 dimensional subspace (“brane”) while gravity is allowed to propagate in all dimensions. Gravity then only appears weak on the standard model brane because it is only felt when gravitons “go through” the brane. Now, since the edges of the extra dimensions are identified by compactification, boundary conditions are generated which lead to quantification of momentum along the extra dimension. Since momentum in those directions looks like mass to observers confined to the brane, and in this scenario many graviton excitations with small mass splittings are present, a Kaluza-Klein tower of gravitons emerges. The coupling of standard model particles to individual gravitons remains very small, but there are so many graviton states that the phase space becomes very large and observable cross-sections ensue. Furthermore, since the graviton couples to the energy-momentum tensor, this impacts all processes.

Two classes of processes can be studied. In the case of direct production of gravitons, the bulk space is involved, and since translational invariance in the directions perpendicular to the standard model brane is broken, momentum in that direction is not conserved. Physically, the graviton escapes into the bulk right after production, leading to a \cancel{E}_T signature. The most sensitive channels are the search for monophoton or monojet events. The other option is to look for high-mass cross-section deviations in standard model processes. Indeed, at high mass the graviton contribution can exceed the standard model one, and furthermore its spin 2 nature can affect the angular distribution of

the outgoing particles. Figure 10 shows the \cancel{E}_T distribution in a CDF search in the monophoton channel (Aaltonen et al., 2008b), and the dielectron and diphoton invariant mass spectrum in a $D\bar{O}$ search for a high mass deviation in dielectron and diphoton events (Abazov et al., 2009b). The limits range from

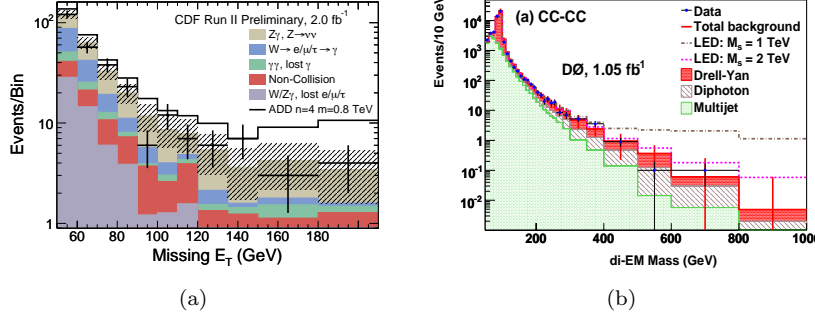


Figure 10. Search for ADD large extra dimensions: (a) \cancel{E}_T distribution in a CDF search in the monophoton channel and (b) dielectron and diphoton mass spectrum in a $D\bar{O}$ interference search.

~ 1.4 to ~ 1 TeV for two to six extra dimensions in the CDF analysis, and ~ 2.1 to ~ 1.3 TeV for two to seven extra dimensions in the $D\bar{O}$ analysis. Note however that these limits are not directly comparable since slightly different formalisms are used.

6.2 RS

A different model has a single extra dimension with a warped metric (Randall and Sundrum, 1999). The standard model fields are still confined to a brane with gravity propagating in the extra dimension, but gravity “originates” on a second brane. The extra dimension is compactified with radius r_c and the two branes are located at $y = r_c\phi = 0, \pi r_c$ along the extra dimension. With the metric warped by a factor $e^{-2kr_c\phi}$, a TeV scale can be generated from a fundamental scale at M_{Pl} if $2kr_c\phi \sim 30$. In this scenario, there are only a few massive graviton excitations, with mass separations corresponding to the zeros of the Bessel function, providing a smoking gun signature for the model if more than one of the excitations can be observed. The lightest excitation is expected to have mass below a few TeV, and the widths of the excitations depend on the warp factor k (Davoudiasl et al., 2001). Also note that since this is a graviton, in contrast to a Z' decays to a pair of photons are allowed. Both CDF (Aaltonen et al., 2007) and $D\bar{O}$ (Abazov et al., 2008c) have search results setting 95% C.L. limits ranging from $m_G > \sim 300$ GeV for $k/M_{Pl} = 0.01$ to $m_G > \sim 900$ GeV for $k/M_{Pl} = 0.1$.

The warped extra dimension model can be augmented by localizing particles along the extra dimension: since scales depend on the position of the

particle wave function, masses are generated by geometry, and mixing angles originate from particle wavefunction overlaps. The heavier fermions and gauge boson excitations are located close to the “infrared” brane with scale 1 TeV where the Higgs boson is also located. Bounds from precision measurements require that the gauge boson excitations have masses in the multi-TeV range, and because these are located close to the IR brane, they mainly couple to the top quark, and W and Z bosons. These gauge boson excitations represent the most promising channels for discovery, but since their couplings to light fermions are small, the production cross-sections are small. In contrast with this, they are expected to be very broad $t\bar{t}$, WW or ZZ resonances (Lillie et al., 2007).

This also leads to a new experimental phenomenology: having very heavy particles decaying to top quarks, W and Z bosons means the latter are produced with momenta much larger than their mass, leading to collimated decay products. For leptonic W and Z boson decays this is manageable, since detectors measure charged lepton directions extremely well, however hadronic decays lead to jets, which are intrinsically relatively wide. This is illustrated in Fig. 11, where the angular ($dR = \sqrt{\Delta\phi^2 + \Delta\eta^2}$) distance between top quark decay products is shown as a function of top quark transverse momentum in simulated decays. Since the typical physical jet radius R_{jet} is ~ 0.5 , for

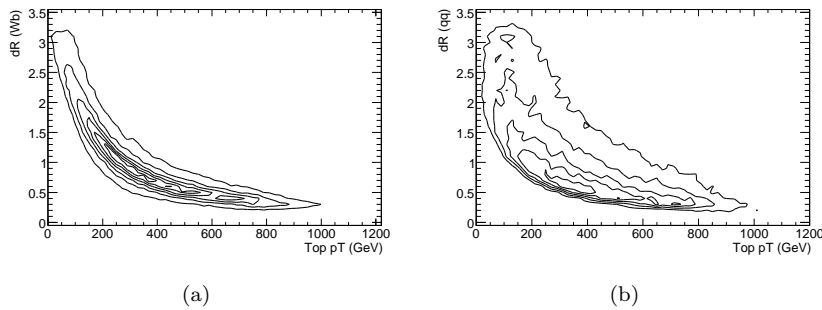


Figure 11. Angular distance between (a) the b quark and W boson and (b) light quarks from hadronic W boson decays as a function of top quark transverse momentum.

top transverse momenta larger than ~ 300 GeV the distance between quarks from W decays starts dropping below $2R_{jet}$, and similarly for the distance between the b quark and the W boson. Hadronically decaying W bosons can then be reconstructed as a single jet, and for leptonic W boson decays, lepton isolation loses its effectiveness as a signal selection variable. But the LHC experiments’ calorimeters have very fine granularity, and resolving the substructure of merged jets can be attempted.

A recent ATLAS study (The ATLAS Collaboration, 2009) has explored this using fully simulated $m = 2, 3$ TeV Z' bosons decaying to top quark

pairs. This covers top quark transverse momenta from 500 to 1500 GeV, with only few events in the “transition region” between 200 and 600 GeV. QCD multijet events with $280 < p_T < 2240$ GeV are used as the main background sample. For the fully hadronic top quarks decays, the fundamental idea is that even though the decay hadrons are reconstructed as a single jet, this jet originates from a massive particle decaying to three hard partons, not one. If it were possible to measure each of the partons in the jet perfectly it would be possible to reconstruct the originator’s invariant mass and its direct daughters. Of course, since quarks radiate and hadronize there is cross-talk, and the detectors cannot resolve the individual partons. However, the invariant mass of all the jet constituents (typically calorimeter cells) can be calculated, and is expected to be $> \sim m_{top}$. This can be seen in the left panel of Fig. 12: the slow increase in jet mass versus top quark p_T is due to increased radiation. The jet mass is not sensitive to jet substructure however, and for single jets from hadronic top quark decays three “concentrations” of energy are expected. There are multiple ways to exploit this, and the ATLAS study uses k_\perp splitting scales (Butterworth et al., 2002). The k_\perp algorithm, a nearest neighbor jet clustering algorithm based on p_T -weighted angular distance, is much better suited to understanding jet substructure than cone-type algorithms which seek to maximize energy in an $\eta \times \phi$ cone. The splitting, or y -scales give the energy scale at which one switches from one to two, two to three, etc. jets. The splitting scale from one to two jets for the signal is given in the right panel of Fig. 12. For the QCD multijet background, both the jet mass and splitting scales take the shape of negative exponential functions. In the study, the jet mass and splitting scales are combined into

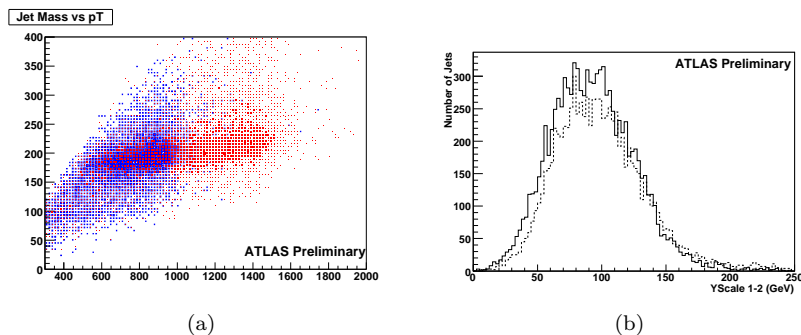


Figure 12. ATLAS study of high- p_T top quark decays: (a) jet mass as a function of top quark p_T , both in GeV, for $m = 2$ (blue) and 3 (red) TeV Z' bosons, and (b) one-to-two jet splitting scale for top quark “monojets” from $m = 2$ (solid) and 3 (dashed) TeV Z' bosons.

a likelihood variable y_L , which is shown for both signal and background as a function of jet p_T in Fig. 13. Signal and background efficiencies depend on the chosen value of the likelihood cut: for 90 (65)% signal efficiency at $p_T = 1$

TeV, the QCD multijet pass rate is 15 (7)%.

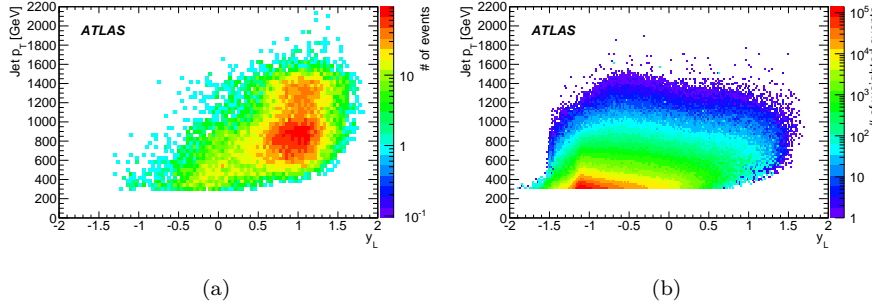


Figure 13. *ATLAS study of high- p_T top quark decays: likelihood value as a function of jet p_T for (a) signal and (b) background.*

In the same analysis, ATLAS also studied semileptonic top quark decays. Since the b -jet is close to the lepton, the usual lepton isolation requirement is ineffective. This is replaced by two variables, $x_\mu = 1 - m_b^2/m_{visible}^2$ (with m_b the mass of the jet near the lepton), which represents the fraction of visible top mass carried away by the muon (Thaler and Wang, 2008), and the relative p_T of the lepton with respect to the jet. The key conclusion from this analysis is that the QCD multijet background can be reduced to almost an order of magnitude less than the irreducible continuum $t\bar{t}$ background. The main challenge in the search for a resonance is then the ability to identify a peak over the background. For narrow resonances, the ATLAS study suggests that a mass resolution of approximately 5% of the resonance mass is achievable.

7 More

Due to the limited time available, many topics were not, or barely addressed. Some of these are:

- Long lived particles, which can decay outside (Abazov et al., 2009c), or halfway out (Abazov et al., 2006; Abazov et al., 2008b; Abazov et al., 2009d) the detector, or come to rest and decay later (Abazov et al., 2007).
- “Quirks” (Kang and Luty, 2009).
- Lepton jets (Cheung et al., 2009).
- R -parity violating supersymmetry (Feng et al., 2009).
- Model-independent searches (Aaltonen et al., 2008a).

8 Conclusions

So far, searches for new particles or interactions have only succeeded in setting stringent constraints on their existence. However, we do expect to see something new in the next few years, as the LHC breaks the TeV barrier. If there is a Higgs boson, does it generate fermion masses? Do new particles stabilize its mass? Can we learn something about the nature of standard model particles from these? If there is no Higgs boson, how is its role fulfilled? Are there new interactions or space dimensions?

We can hope for a very rich phenomenology which will help us understand more than the question of particle masses, so that we can not only have the particle physics equivalent of Mendeleev's table, but also understand how its structure comes about. This may require a new paradigm shift, as during the emergence of the quark model.

Acknowledgments

The author would like to thank the organizers of the school for a wonderful time at St. Andrews. From my colleagues' excellent lectures to haggis and stimulating discussions, it was an experience I will remember fondly.

Bibliography

- Aad, G. et al.: 2009, *eprint* 0901.0512
- Aaltonen, T. et al.: 2007, *Phys. Rev. Lett.* **99**, 171801
- Aaltonen, T. et al.: 2008a, *Phys. Rev.* **D78**, 012002
- Aaltonen, T. et al.: 2008b, *Phys. Rev. Lett.* **101**, 181602
- Aaltonen, T. et al.: 2009a, *Phys. Rev. Lett.* **102**, 031801
- Aaltonen, T. et al.: 2009b, *Phys. Rev.* **D79**, 112002
- Aaltonen, T. et al.: 2009c, *Phys. Rev. Lett.* **103**, 041801
- Abazov, V. M. et al.: 2004, *Phys. Rev.* **D69**, 111101
- Abazov, V. M. et al.: 2006, *Phys. Rev. Lett.* **97**, 161802
- Abazov, V. M. et al.: 2007, *Phys. Rev. Lett.* **99**, 131801
- Abazov, V. M. et al.: 2008a, *Phys. Lett.* **B669**, 278
- Abazov, V. M. et al.: 2008b, *Phys. Rev. Lett.* **101**, 111802
- Abazov, V. M. et al.: 2008c, *Phys. Rev. Lett.* **100**, 091802
- Abazov, V. M. et al.: 2008d, *Phys. Lett.* **B660**, 449
- Abazov, V. M. et al.: 2008e, *Phys. Rev. Lett.* **100**, 211803
- Abazov, V. M. et al.: 2009a, *Phys. Lett.* **B680**, 34
- Abazov, V. M. et al.: 2009b, *Phys. Rev. Lett.* **102**, 051601
- Abazov, V. M. et al.: 2009c, *Phys. Rev. Lett.* **102**, 161802
- Abazov, V. M. et al.: 2009d, *Phys. Rev. Lett.* **103**, 071801
- Alcaraz, J. et al.: 2007, *eprint* hep-ex/0712.0929
- Antoniadis, I.: 1990, *Phys. Lett.* **B246**, 377
- Arkani-Hamed, N., Dimopoulos, S., and Dvali, G. R.: 1998, *Phys. Lett.* **B429**, 263
- Balazs, C. and Yuan, C. P.: 1997, *Phys. Rev.* **D56**, 5558
- Butterworth, J. M., Cox, B. E., and Forshaw, J. R.: 2002, *Phys. Rev.* **D65**, 096014
- Campbell, J. M. and Ellis, R. K.: 2002, *Phys. Rev.* **D65**, 113007
- Cheung, C., Ruderman, J. T., Wang, L.-T., and Yavin, I.: 2009, *eprint* 0909.0290
- Corcella, G. et al.: 2001, *JHEP* **01**, 010
- Davoudiasl, H., Hewett, J. L., and Rizzo, T. G.: 2001, *Phys. Rev.* **D63**, 075004
- de Roeck, A., Ball, A., Della Negra, M., Fo, L., and Petrilli, A.: 2006, *CMS physics: Technical Design Report*, Technical Design Report CMS, CERN, Geneva, revised version submitted on 2006-09-22 17:44:47
- Englert, F. and Brout, R.: 1964, *Phys. Rev. Lett.* **13**, 321
- Feng, J. L., Grivaz, J.-F., and Nachtman, J.: 2009, *eprint* 0903.0046
- Ferrari, A. and Collot, J.: 2000, *Sensitivity study for a Z' boson decaying*

- into two right-handed Majorana neutrinos at LHC in the ATLAS detector, Technical Report ATL-PHYS-2000-034, CERN, Geneva, revised version number 1 submitted on 2000-12-20 16:29:22
- Frixione, S., Nason, P., and Ridolfi, G.: 2007, *eprint* 0707.3081
- Frixione, S. and Webber, B. R.: 2002, *JHEP* **06**, 029
- Gleisberg, T. et al.: 2009, *JHEP* **02**, 007
- Guralnik, G. S., Hagen, C. R., and Kibble, T. W. B.: 1964, *Phys. Rev. Lett.* **13**, 585
- Henriques, A. and Poggioli, L.: 1992, *Detection of the Z' vector boson in the jet decay mode ($Z' \rightarrow q\bar{q} \rightarrow jj$). Resolution and pile-up studies*, Technical Report ATL-PHYS-92-010. ATL-GE-PN-10, CERN, Geneva
- Higgs, P. W.: 1964a, *Phys. Rev. Lett.* **13**, 508
- Higgs, P. W.: 1964b, *Phys. Lett.* **12**, 132
- Higgs, P. W.: 1966, *Phys. Rev.* **145**, 1156
- Kang, J. and Luty, M. A.: 2009, *JHEP* **11**, 065
- Langacker, P.: 2008, *eprint* 0801.1345
- Lee, B. W., Quigg, C., and Thacker, H. B.: 1977, *Phys. Rev.* **D16**, 1519
- Lester, C. G. and Summers, D. J.: 1999, *Phys. Lett.* **B463**, 99
- Lillie, B., Randall, L., and Wang, L.-T.: 2007, *JHEP* **09**, 074
- Mangano, M. L., Moretti, M., Piccinini, F., Pittau, R., and Polosa, A. D.: 2003, *JHEP* **07**, 001
- Mehdiyev, R., Siodmok, A., Sultansoy, S., and Unel, G.: 2008, *Eur. Phys. J.* **C54**, 507
- Polesello, G. and Tovey, D. R.: 2009, *eprint* 0910.0174
- Randall, L. and Sundrum, R.: 1999, *Phys. Rev. Lett.* **83**, 3370
- Rizzo, T. G.: 2006, *eprint* hep-ph/0610104
- Rizzo, T. G.: 2007, *JHEP* **05**, 037
- Sagan, C.: 1980, *Cosmos*, Random House, New York, 1st edition
- Sjostrand, T., Mrenna, S., and Skands, P.: 2006, *JHEP* **05**, 026
- Thaler, J. and Wang, L.-T.: 2008, *JHEP* **07**, 092
- The ATLAS Collaboration: 2009, *Reconstruction of High Mass $t\bar{t}$ Resonances in the Lepton+Jets Channel*, Technical Report ATL-PHYS-PUB-2009-081. ATL-COM-PHYS-2009-255, CERN, Geneva
- The CDF and D0 Collaborations: 2009, *eprint* 0911.3930
- The D0 Collaboration: 2009a, *Search for Higgs boson production in dilepton plus missing transverse energy final states with 5.4 fb⁻¹ of $p\bar{p}$ collisions at $\sqrt{s}=1.96$ TeV*, Technical Report DØ Conference Note 6006-CONF
- The D0 Collaboration: 2009b, *Search for pair production of the supersymmetric partner of the top quark in the $e+\mu+b+b(\bar{b})+MET$ decay channel at D0*, Technical Report DØ Conference Note 5937-CONF
- The LEP and SLD Collaborations: 2006, *Phys. Rept.* **427**, 257